

AN AUTOMATIC CALIBRATION METHOD BASED ON FEATURE POINT MATCHING FOR THE COOPERATION OF WIDE-ANGLE AND PAN-TILT-ZOOM CAMERAS

Hsien-Chou Liao, Ming-Ho Pan, Hung-Wei Hwang, Min-Chih Chang, Po-Cheng Chen

*Chaoyang University of Technology, Department of Computer Science and Information Engineering
168 Jifong E. Rd., Wufong Township Taichung County, 41349, Taiwan (R.O.C.)
e-mail: hcliao@cyut.edu.tw, s9527153@cyut.edu.tw, s9527174@cyut.edu.tw, s9527126@cyut.edu.tw,
s9527039@cyut.edu.tw*

crossref <http://dx.doi.org/10.5755/j01.itc.40.1.191>

Abstract. Wide-angle cameras are used to monitor large open areas, but moving objects on the image are often too small to view in detail. However, pan-tilt-zoom (PTZ) cameras have zooming capabilities that can be used to capture close-up images of a moving object. Therefore, the cooperation of these two types of cameras has been studied extensively in recent years. A calibration method is necessary to achieve the above cooperation. For any coordinate on the image plane of a wide-angle camera, this calibration method is needed to obtain the corresponding pan, tilt, and zoom values, known as the point correspondence of the PTZ camera. It is inconvenient to manually establish point correspondences, as shown in previous studies. Therefore, an automatic calibration method is proposed in this paper. The method is mainly based on the matching of feature points on the images of wide-angle and PTZ cameras. A feature point (FP) is extracted based on several edge operators derived from a 2D Gaussian smoothing function. A two-phase FP match is then designed to obtain the point correspondences. In the study of a prototype for capturing close-up images of moving objects, the calibration process took approximately 7 minutes for 44 FPs. The average successful rate of the capturing tasks was 82 percent. It shows that the automatic calibration method is feasible for the cooperation of wide-angle and PTZ cameras.

Keywords: dual-camera system, surveillance system, motion detection, moving object tracking, ubiquitous camera.

1. Introduction

The development of embedded systems and wireless communication has caused IP-based cameras and IP-based surveillance systems to become popular. Unlike traditional digital cameras without computing capability, IP-based cameras usually have an embedded Linux system. They can operate individually and provide some basic services, such as motion detection or object tracking. IP-based cameras can be classified into three categories. One is the passive, i.e., wide-angle camera, which is used to monitor a fixed area with a fixed focal lens. Another is the active, i.e., pan-tilt-zoom (PTZ) camera, which is capable of increasing the monitoring area and enhancing the image quality. The last is designed for special purposes, such as Omni directional cameras or thermal cameras. The Internet connection increases the accessibility of IP-based cameras. The cooperation of multiple cameras has been studied recently for new services, such as consistent object labeling[1-2], pedestrian tracking, behavior analysis and so on. For the surveillance of large open areas, the objects in the image of a wide-angle camera may be too small to recognize. A PTZ

camera can be used to capture a close-up image of an object. However, its field of view (FOV) is limited when zooming in on a specific target. Therefore, the cooperation of wide-angle and PTZ cameras is complementary. This has been extensively studied recent years [3-7]. The cooperation scenario is shown in Figure 1. When an object appears in the image of a wide-angle camera, as shown in Figure 1(a), the PTZ camera can be controlled to capture a close-up image of the object, as shown in Figure 1(b).

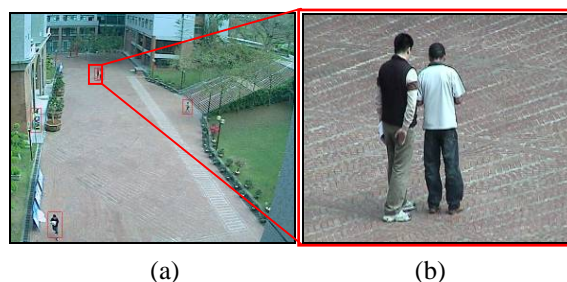


Figure 1. Cooperation scenario of wide-angle and PTZ cameras: (a) an object on the image of a wide-angle camera, (b) the close-up image captured by a PTZ camera

It is very difficult for surveillance to manually capture close-up images of all objects passing through an open area. An automatic system is needed. In order to achieve the cooperation of wide-angle and PTZ cameras, camera calibration is the key process. For the coordinate of a specific object in the image of a wide-angle camera, the calibration calculates the corresponding pan, tilt, and zoom values needed to control the PTZ camera and capture the close-up image. In this paper, an automatic calibration method is proposed and a prototype system is also presented to achieve the above task. The calibration is based on the feature points (FPs) extracted by using a 2D Gaussian smoothing function [8]. Next, the corresponding pan and tilt values are obtained automatically using two phases: wide-angle FP matching and zoom-in FP matching. The zoom value is computed based on the height of the object. The established FP and pan/tilt correspondences are in the prototype.

The remainder of this paper is organized as follows: Section 2 reviews related works; Section 3 presents the automatic calibration method; Section 4 presents the computation of pan, tilt, and zoom values; Section 5 describes the prototype and the experimental study; Section 6 presents the conclusion indicated by this study.

2. Related Works

The calibration method of cameras is important for the cooperation of multiple cameras. Methods described in previous studies can be classified into three categories:

- (1) *3D world coordinate system*: This category is based on a common 3D world coordinate system for multiple cameras to compute the desired pan and tilt angles of PTZ cameras [9]. R. Bodor et al. proposed a dual camera system for activity recognition [10]. The calibration is based on the inverse kinematics for computing pan and tilt angles from the 3D world coordinate. Marchesotti et al. also proposed a dual-camera system for face detection [11-12]. The calibration method is based on the Tsai's method [13]. At least 12 pairs of 2D image plane and 3D world coordinates are needed to achieve precise calibration. Menudet et al. proposed a similar self-calibration method based on the image plane [14].
- (2) *Scene-dependent*: This category is depended on specific features in the scene. Song and Tai proposed a calibration method for traffic monitoring [15], mainly based on parallel lane markings and lane width to compute the camera parameters. Lv et al. proposed a self-calibration method using vertical line segments of the same height [16]. Chen and Wang proposed a novel and efficient method for the calibration of multiple PTZ cameras [3] mounted on the ceiling of an indoor environment. The calibration is based on the tilt angle and altitude of the PTZ cameras. The image

processing technique is also used to infer the relative positioning and orientation among multiple PTZ cameras. However, the calibration method cannot be adapted to different PTZ camera installations or configurations.

- (3) *Ad hoc technique*: This category utilizes special techniques for camera calibration. Xing et al. proposed a calibration method based on a genetic algorithm [17]. Tresadern and Reid proposed a calibration based on human motion [18]. Davis and Chen proposed a more complete calibration method for pan-tilt cameras, using an improved camera model to provide a large virtual calibration target by tracking the motion of an LED point feature [19]. However, it is troublesome to obtain the calibration data for different models of cameras. Lee et al. also proposed a manual calibration method [20]. An image registration technique is used to establish panning, tilting, and zooming tables separately. However, the construction of the pan/tilt/zoom tables is still in convenient for different models of cameras. In a previous study by this researcher, a manual calibration method was proposed [21]. However, the problem still exists.

A number of disadvantages are mentioned in the previous studies. Therefore, an automatic calibration method is proposed simply based on the 2D image plane without considering the 3D world coordinate system. It is also scene-independent and general for the cooperation of wide-angle and PTZ cameras.

3. Automatic calibration method

When a wide-angle camera and a PTZ camera are calibrated, the corresponding pan, tilt, and zoom values can be obtained for any given coordinate on the image plane of a wide-angle camera. Therefore, when a moving object appears on the image plane of a wide-angle camera, the obtained pan/tilt/zoom values can be used to control the PTZ camera to focus on the object. An automatic calibration method is designed to establish a set of point correspondences for obtaining the desired pan, tilt, and zoom values. The computation of the desired pan and tilt values is differed from that of the zoom value since the zoom value is related to the size of the object.

The calibration of the pan and tilt values is presented firstly. The process is shown in Figure 2. The main principle of the process is based on the FPs on the images of the wide-angle and PTZ cameras. If the corresponding pan and tilt values of every FP are obtained, they can be deemed as a point correspondence. The process consists of two phases: wide-angle FP matching and zoom-in FP matching. In the wide-angle FP matching phase, the PTZ camera is zoomed out to the maximum wide-angle. The real-time images are captured simultaneously from two cameras. The FPs on two images are extracted based on a 2D Gaussian smoothing function, which is presented later.

Next, a normalized cross correlation (NCC) method is used to match the FPs on two images. A false match is also eliminated to establish the set of FP pairs. After this phase, a set of reference FPs in the image of the wide-angle camera and the corresponding FPs in the image of the PTZ camera in the maximum wide-angle mode is established.

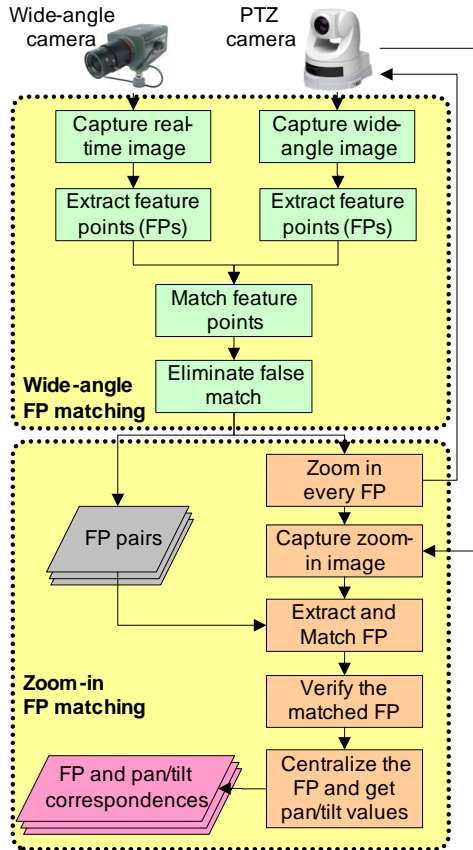


Figure 2. The process of the proposed automatic calibration method for pan/tilt values

The second phase is zoom-in FP matching. The purpose is to obtain the corresponding pan and tilt value of the FP in every FP pair. Assume two FPs of one FP pair are denoted as PW_i and PP_i to represent the FP on the image of wide-angle camera and the PTZ camera, respectively. Firstly, the PTZ camera is controlled to centralize and zoom in on PP_i . However, minor errors may exist while zooming, since a position on the wide-angle image is mapped into a rectangular area on the zoom-in image. In order to get precise pan and tilt values, a set of new FPs in the zoom-in image are extracted and matched with PW_i . Assume the new matched FP is denoted as PP'_i . It should be within a pre-defined central area; otherwise, it is discarded. If PP'_i satisfies such criteria, the PTZ camera is controlled to centralize on PP'_i and get the corresponding pan and tilt values from the PTZ camera. They are the desired correspondences of PW_i . After the above process, a set of point correspondences (FPs) in the image of the wide-angle camera and their corresponding pan and tilt values are established automatically.

The key steps of the above process, including the feature point extraction, matching, false matching elimination, and zoom-in FP matching are presented illustratively as follows.

(1) Feature point extraction

An FP is a point of human interest in an image, such as an intersection of two lines, a corner, and so on. In this paper, the set of FPs is extracted based on the method presented in [10]. Several edge operators are used to extract FPs. For a specific position (x, y) on an image, the first partial derivatives of the 2D Gaussian smoothing function in x and y directions are denoted as G_x^σ and G_y^σ , respectively. They are computed by using Eq. (1):

$$G_x^\sigma(x, y) = -\frac{x}{\sigma^2} \exp\left(-\frac{x^2 + y^2}{2\sigma^2}\right), \quad (1)$$

$$G_y^\sigma(x, y) = -\frac{y}{\sigma^2} \exp\left(-\frac{x^2 + y^2}{2\sigma^2}\right),$$

where σ is the standard deviation of the associated probability distribution. It is set to 2 for noise suppression. The gradients of an image $I(x, y)$ smoothing by $G_x^\sigma(x, y)$ and $G_y^\sigma(x, y)$ in the x and y directions can be computed by using Eq. (2):

$$I_x^\sigma(x, y) = I * G_x^\sigma(x, y) \quad (2)$$

$$I_y^\sigma(x, y) = I * G_y^\sigma(x, y)$$

The operator $*$ is a convolution operation. The modulus of the gradient vector of $I(x, y)$ can be computed by using Eq. (3):

$$|\nabla I^\sigma(x, y)| = \sqrt{|I_x^\sigma(x, y)|^2 + |I_y^\sigma(x, y)|^2}. \quad (3)$$

The position (x, y) is a feature point when it satisfies two conditions. The first condition is that the value $|\nabla I^\sigma(x, y)|$ is larger than a pre-defined threshold of 20. The second condition is that $|\nabla I^\sigma(x, y)|$ is the local maxima within a pre-defined area of 27×27 .

According to the above method, an example of extracted FPs is shown in Figure 3 and marked with a red cross.



Figure 3. An example of feature point extraction

(2) Feature point matching

Two sets of FPs are extracted separately from the image of the wide-angle camera and the wide-angle image of the PTZ camera. Next, a normalized cross correlation (NCC) method is used for FP matching. NCC is commonly used as a metric to evaluate the similarity of FPs in two sets. An example of FP matching is shown in Figure 4. The matched FP has the same number as shown in Figures 4(a) and 4(b).

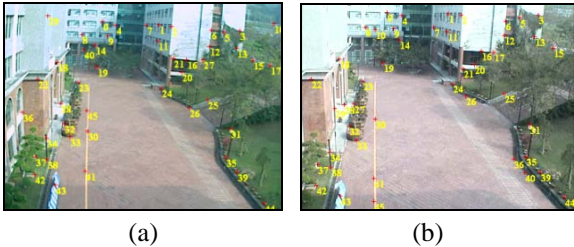


Figure 4. An example of feature point matching:
 (a) the image of the wide-angle camera,
 (b) the image of the PTZ camera

(3) False match elimination

The set of FP pairs matched using NCC may contain false matches (such as FPs No. 21 and 26 in Figure 4). These false matches cannot be point correspondences and must be eliminated. The elimination is based on their geometric relationship. The above example after false match elimination is shown in Figure 5.



Figure 5. An example of false match elimination:
 (a) the image of the wide-angle camera,
 (b) the image of the PTZ camera

(4) Zoom-in FP matching

In this step, the corresponding pan and tilt values of every FP pair are obtained using the above FP matching technique with the zoom-in image of the PTZ camera. For matched FP pair PW_i and PP_i , the PTZ is controlled to zoom in on the PP_i to capture a close-up image of the area around it. New FPs in the zoom-in image are extracted. Then, PW_i is matched with the new FPs to find the new matched FP, PP'_i . An example of zoom-in FP matching is shown in Figure 6. In Figure 6(a), the original size of the image containing PW_i is shown on the right-hand side. The zoom-in image of PP_i is shown in Figure 6(b). The red dot is the matched PP'_i . It is the ideal condition where PP'_i is in the precise center of the zoom-in image.

The new matched FP, PP'_i , is verified to ensure there is no possible false match. In general, if the PTZ camera is controlled to centralize and zoom in on PP_i ,

the matched PP'_i should be within the central area. Otherwise, PP'_i is a false match. An example is shown in Figure 7 to illustrate the verification of PP'_i . In Figure 7(a), the yellow cross is the center of the image. Assume the matched PP'_i is marked with a red cross and is within the red-dashed pre-defined circle. The PTZ camera is controlled to centralize PP'_i again and overlap it with the center of the image as shown in Figure 7(b). If PP'_i is not within the pre-defined circle as shown in Figure 7(c), it is a false matching and discarded.

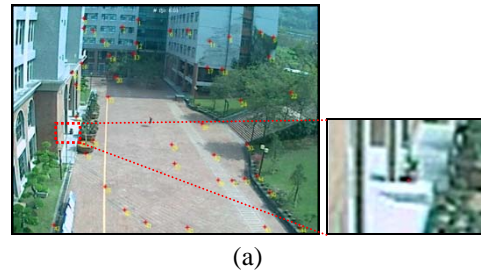


Figure 6. An example of zoom-in FP matching:(a) the image containing the FP in its original size,(b)the corresponding zoom-in image of the PTZ camera

When the PP'_i is centralized as shown in Figure 7(b), the pan and tilt values of the PTZ camera are recorded with PW_i as a point correspondence. These point correspondences are the final result of the automatic calibration method. They are used to compute the desired pan and tilt values for any given coordinate on the image plane of the wide-angle camera.

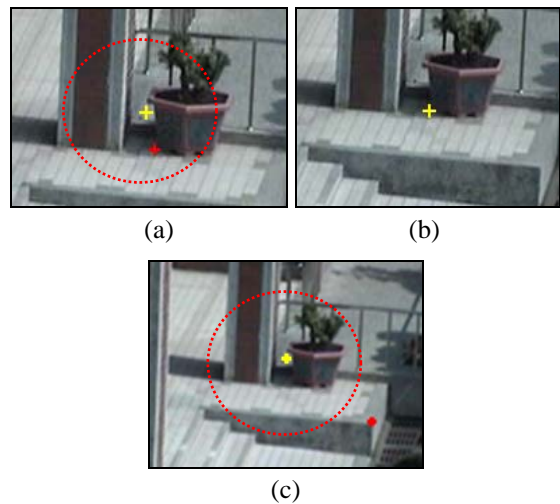


Figure 7. The demonstration of FP verification: (a) the matched FP (red) and the center of the image (yellow), (b) FP is centralized, (c) the matched FP is not in the center area

4. The computation of pan/tilt/zoom values

For an object in the image of the wide-angle camera, assume its position (x', y') and size (w', h') can be known. Its position is used to compute the corresponding pan and tilt values for the PTZ camera, based on the set of point correspondences established using the automatic calibration process. The object size is used to compute the suitable zoom values. In order to compute the desired pan and tilt values, (x', y') is assumed to the next possible position of a moving object. It is marked with a blue-dashed rectangle, as shown in Figure 8. Next, the closest FPs of point correspondences to (x', y') in the vertical and horizontal line are found separately and denoted as (x_1, y_1) and (x_2, y_2) . Assume the corresponding pan and tilt values for (x_1, y_1) and (x_2, y_2) are (p_1, t_1) and (p_2, t_2) , respectively. The desired pan and tilt values, (p', t') , for (x', y') are computed based on a trigonometric formula, as shown in Eq. (4):

$$p' = (x' - x_1) \times \left(\frac{p_1 - p_2}{x_1 - x_2} \right) + p_1 \quad (4)$$

$$t' = -(y' - y_1) \times \left(\frac{t_1 - t_2}{y_1 - y_2} \right) + t_1$$

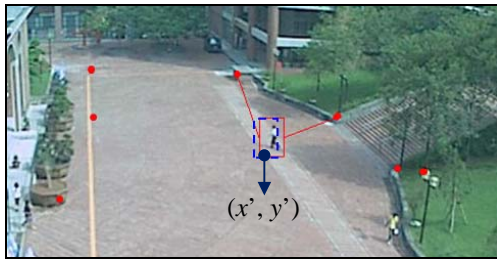


Figure 8. The computation of pan/tilt values

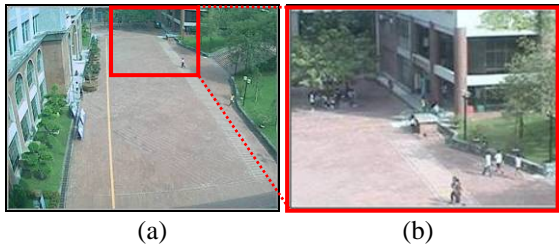


Figure 9. An example of measuring zoom-in image size:
(a) wide-angle image (zoom=1),
(b) the zoom-in image (zoom=5,000)

In advance, the computation of the zoom value is according to the size of the moving object. Before the computation, a look-up table is first established. For the physical zoom values (1 to 14,000 for an AXIS-215 PTZ camera), the zoom-in image sizes are recorded every 500 increments. An example is used to illustrate the measurement of the zoom-in image size as shown in Figure 9. Figure 9(a) is the wide-angle image with the zoom value set to 1. Figure 9(b) shows the zoom value set to 5000. It is only a partial view of the wide-angle image, and is marked by a red rectangle. Next, the height of the rectangle in Figure 9(a) is recorded in the look-up table. A partial look-up table

is listed in Table 1. Only the height is considered here, since the main target is a person in an open area. The height of a person is usually larger than its width.

According to such a look-up table, a suitable zoom value can be computed for a specific object height. Assume the height of a moving object is denoted as h' . The pre-defined ratio of the zoom-in image to an object is denoted as R . $R \times h'$ is the expected height of the zoom-in image. It can be found between two heights in the look-up table, denoted as h_1 and h_2 ($h_1 \leq h_2$). The corresponding zoom values are denoted as z_1 and z_2 . The desired zoom value z' is computed using the following equation.

$$z' = (R \times h' - h_1) \times \left(\frac{z_2 - z_1}{h_2 - h_1} \right) + z_1 \quad (5)$$

Table 1. A partial look-up table of the zoom value

Zoom	Height
14000	9
13500	10
13000	12
12500	14
12000	16
...	...

5. The prototype system

A prototype system was implemented using Visual C# 2008. It is designed for capturing close-up images of every object passing through an open area. The system consists of one wide-angle camera and multiple PTZ cameras. The automatic calibration process is performed individually on every PTZ camera to establish the point correspondences. The screenshot of the automatic calibration tool is shown in Figure 10. The image of the wide-angle camera is shown on the left-hand side. The image of the PTZ camera is shown on the right-hand side. Numerous FPs are marked on the wide-angle image. The FP circled in red denotes it being in the zoom-in FP matching phase. The corresponding FP on the zoom-in image is shown on the right-hand side. There are 51 FPs in total, with 14 FPs finished and one FP failing to pass the verification step shown at the bottom of the tool.



Figure 10. Automatic calibration tool screenshot

After the calibration process is finished, the prototype system can perform the automatic close-up image capturing task. The screenshot is shown in Figure 11. The real-time image of the wide-angle camera is shown in the upper-right part. The moving objects are detected based on the background subtraction technique, and are marked with different colors to represent their status. An object marked with a red, yellow, or blue rectangle denotes its close-up image as being uncaptured, capturing, and captured, respectively. The real-time image of the PTZ camera is displayed at the top of the images on the right-hand side. The images under the real-time image of the PTZ camera are continuous shots of a moving object. When the PTZ camera is rotating or the object is moving, the image may be blurred. Continuous shots enable at least two clear images to be found among all the shots. The actual size of the images is 640×480 pixels. The first four images of the five continuous shots are displayed on the user interface. The continuous shots of two objects are shown in Figure 12.



Figure 11. Screenshot of the prototype system



Figure 12. Two examples of continuous shots: (a) vertical movement, (b) horizontal movement

In advance, two experiments were designed to evaluate the performance of the prototype. The first experiment was to measure the elapsed time of the automatic calibration tool. The time is influenced by the number of FPs. In the experiment, there were 44 FPs and the elapsed time was approximately 7 minutes. However, only one click was required to activate the calibration process, meaning the time required was very short. Conversely, manual calibration requires 14 minutes for the same number of FPs. The

above result shows that the automatic calibration process has improved efficiency.

In the second experiment, the system performed close-up image capturing tasks at two different time periods: normal and rush hour. A capturing task is classified into success or failure as defined below:

- *Success*: If the head of a moving object appears completely in one of the continuous shots, the task is classified as a success.
- *Failure*: If either the head of a moving object is not captured, or no moving object exists in any of the continuous shots, the task is classified as a failure.

Additionally, the same checking step presented in the researchers' previous study was used to examine whether a task was failure 0. If the checking result of the continuous shots fails, the system will repeat the capturing task until either the task is successful or the object leaves the FOV of the wide-angle camera. The experimental results are listed in Table 2. The number of objects at normal and rush hour for 20 minutes were 173 and 312, respectively. The success percent at normal and rush hour was 82.6 and 80.4 percent, respectively. The average number of captures per object was computed based on the repeat count, and was 1.53 and 1.42 at normal and rush hours, respectively.

Compared with the researchers' earlier prototype using manual calibration methods during the normal hour period, the success rate of 82.6 percent was lower than that of the previous study (87.8 percent). However, at 1.53 times, the average number of captures per object was better than that of the previous study (2.59 times). This shows that the point correspondences established using the automatic calibration method are precise and useful for close-up image capturing tasks.

Table 2. The results of moving object capturing tasks

Categories	Periods	
	Normal Hour	Rush Hour
Number of objects	173	312
Success	143 (82.6%)	259 (80.4%)
Repeat	92	132
Average number of captures per object	1.53 (265/173)	1.42 (444/312)

6. Conclusions

IP-based cameras are becoming more and more popular. This trend simplifies the cooperation of various kinds of cameras. In this paper, an automatic calibration method was proposed for the cooperation of wide-angle cameras and PTZ cameras. The calibration method was mainly based on the FPs detected using a 2D Gaussian smoothing function. A prototype was implemented to fulfill the automatic calibration method for a close-up image capturing task in an open area. The calibration process can be finished quickly with one click. After the point correspondences are

established, the desired pan and tilt values can be computed for any given coordinate on the image of the wide-angle camera. According to the experiment, the success rate of close-up image captures was 82.6 percent. If the success rate is expected to improve further, the predictions of the moving object positions and the elapsed time of camera rotation are two main factors that need to be considered. The prototype can also be refined to provide different tasks for different situations. For example, close-up image capturing tasks are suitable for a large numbers of moving objects in an open area. However, tracking tasks are suitable for small numbers of moving objects during specific periods of time. The prototype can be context-aware and switch its task automatically.

Acknowledgement

This work was funded by the National Science Council under grant NSC97-2815-C-324-009-E.

References

- [1] **S. Khan, M. Shah.** Consistent labeling of tracked objects in multiple cameras with overlapping fields of view, *IEEE Transactions on Pattern Analysis and Machine Intelligence*, Vol.25, Oct. 2003, 1355-1360.
- [2] **S. Calderara, A. Prati, R. Vezzani, R. Cucchiara.** Consistent labeling for multi-camera object tracking, *Lecture Notes in Computer Science*, Vol.3617, 2005, pp. 1206-1214.
- [3] **I.H. Chenand, S.J. Wang.** Efficient vision-based calibration for visual surveillance systems with multiple PTZ cameras. *Proceedings of IEEE International Conference on Computer Vision Systems (ICVS 2006)*, 4-7 Jan. 2006, 24-24.
- [4] **S. Khan, O. Javed, Z. Rasheed, M. Shah.** Human tracking in multiple cameras. *Proceedings of Eighth IEEE International Conference on Computer Vision (ICCV 2001)*, 2001, Vol.1, 331-336.
- [5] **Z. Tao, M. Aggarwal, R. Kumar, H. Sawhney.** Real-time wide area multi-camera stereo tracking. *Proceedings of IEEE Computer Society Conference on Computer Vision and Pattern Recognition*, 20-25 June, 2005, Vol.1, 976-983.
- [6] **C. Micheloni, G.L. Foresti, L. Snidaro.** A network of co-operative cameras for visual surveillance. *IEEE Proceedings of Vision, Image and Signal Processing*, 8 April, 2005, Vol.152, 205-212.
- [7] **R. Yi, D. Xu, G. Junbin, M. Antolovich.** Novel methods for high-resolution facial image capture using calibrated PTZ and static cameras. *Proceedings of IEEE International Conference on Multimedia and Expo*, 23 June, 2008, 45-48.
- [8] **J.W. Hsieh.** Fast stitching algorithm for moving object detection and mosaic construction. *Image and Vision Computing*, Vol.22, 2004, 291-306.
- [9] **T.S. Shen, C.H. Menq.** Automatic camera calibration for a multiple-sensor integrated coordinate measurement system. *IEEE Transactions on Robotics and Automation*, Vol.17, No.4, 2001, 502-507.
- [10] **R. Bodor, R. Morlok, N. Papanikolopoulos.** Dual-camera system for multi-level activity recognition. *Proceedings of 2004 IEEE/RSJ International Conference on Intelligent Robots and Systems (IROS 2004)*, Vol.1, Sendai, Japan, 28 September-2 October 2004, 643-648.
- [11] **L. Marchesotti, L. Marcenaro, C. Regazzoni.** A multi-resolution outdoor dual camera system for robust video-event metadata extraction. *Proceedings of 2002 International Conference on Information Fusion*, Vol.2, Italy, 8-11 July 2002, 1184-1189.
- [12] **L. Marchesotti, L. Marcenaro, C. Regazzoni.** Dual camera system for face detection in unconstrained environments. *Proceedings of 2003 International Conference on Image Processing (ICIP 2003)*, Vol.1, Italy, 14-17 September 2003, 1-681-684.
- [13] **R.Y. Tsai.** A versatile camera calibration technique for high-accuracy 3D machine vision metrology using off-the-shelf TV cameras and lenses. *IEEE Journal of Robotics and Automation*, RA-3(4), Aug. 1987, 323-344.
- [14] **J.F. Menudet, J.M. Becker, T. Fournel, C. Mennesier.** Plane-based camera self-calibration by metric rectification of images. *Image and Vision Computing*, Vol.26, No.7, 2 July 2008, 913-934.
- [15] **K.T. Song, J.C. Tai.** Dynamic calibration of pan-tilt-zoom cameras for traffic monitoring. *IEEE Transactions on Systems, Man, and Cybernetics-Part B: Cybernetics*, Vol.36, No.5, 2006, 1091-1103.
- [16] **F. Lv, T. Zhao, R. Nevatia.** Camera calibration from video of a walking human. *IEEE Transactions on Pattern Analysis and Machine Intelligence*, Vol.28, No.9, Sept. 2006, 1513-1518.
- [17] **Y. Xing, Q. Liu, J. Sun, L. Hu.** Camera calibration based on improved genetic algorithm. *Proceedings of IEEE International Conference on automation and logistics*, 18-21 Aug. 2007, 2596-2601.
- [18] **P.A. Tresadern, I.D. Reid.** Camera calibration from human motion. *Image and Vision Computing*, Vol.26, No.6, June 2008, 851-862.
- [19] **J. Davis, X. Chen.** Calibrating pan-tilt cameras in wide-area surveillance networks. *Proceedings of the Ninth IEEE International Conference on Computer Vision (ICCV)*, Vol.1, Nice, France, 14-17 October 2003, 144-149.
- [20] **C.H. Lee, M.G. Wen, C.C. Han, D.C. Kou.** An automatic monitoring approach for unsupervised parking lots in the outdoors. *Proceedings of the 39th Annual 2005 International Carnahan Conference on Security Technology (CCST'05)*, 11-14 Oct. 2005, 271-274.
- [21] **H.C. Liao, Y.C. Cho.** A new calibration method and its application for the cooperation of wide-angle and pan-tilt-zoom cameras. *Information Technology Journal*, Vol.7, No.8, 2008, 1096-1105.

Received August 2010.